Attenuation of cryocooler induced vibration using multimodal tuned dynamic absorbers

Alexander Veprik [a], Vladimir Babitsky[b], Avi Tuito[c]

[a] SemiConductor Devices POB 2250, Haifa 31021, Israel
[b]Loughborough University, Epinal Way, Loughborough, LE11 3TU, UK
[c] Israel Ministry of Defense, Kirya, Tel Aviv, 64734, Israel

ABSTRACT

Modern infrared imagers often rely on split Stirling linear cryocoolers comprising compressor and expander, the relative position of which is governed by the optical design and packaging constraints. A force couple generated by imbalanced reciprocation of moving components inside both compressor and expander result in cryocooler induced vibration comprising angular and translational tonal components manifesting itself in the form of line of sight jitter and dynamic defocusing.

Since linear cryocooler is usually driven at a fixed and precisely adjustable frequency, a tuned dynamic absorber is a well suited tool for vibration control. It is traditionally made in the form of lightweight single degree of freedom undamped mechanical resonator, the frequency of which is essentially matched with the driving frequency or vice versa. Unfortunately, the performance of such a traditional approach is limited in terms of simultaneous attenuating translational and angular components of cooler induced vibration.

The authors are enhancing the traditional concept and consider multimodal tuned dynamic absorber made in the form of weakly damped mechanical resonator, where the frequencies of useful dynamic modes are essentially matched with the driving frequency. Dynamic analysis and experimental testing show that the dynamic reactions (forces and moments) produced by such a device may simultaneously attenuate both translational and angular components of cryocooler-induced vibration. The authors are considering different embodiments and their suitability for different packaging concepts. The outcomes of theoretical predictions are supported by full scale experimentation.

Keywords: cryocooler, infrared imager, vibration, line of sight jitter, multimodal tuned dynamic absorber

1. INTRODUCTION

Split Stirling linear micro-miniature cryocoolers find wide use in infrared (IR) night vision imagers. Such a cryocooler usually comprises electro-dynamically actuated linear pressure wave generator (compressor) and pneumatically actuated resonant expander, which are fixedly mounted upon a common frame and interconnected by a configurable transfer line.

The compressor provides required pressure and volumetric reciprocal change of the working agent (Helium, typically) in the compression and expansion chambers of such a cryoogenic cooler, these chambers are separated by the movable regenerative heat exchanger. The resonating displacer shuttles the working agent back and forth from the cold side to the warm side of the cooler. Because of the favorable phase lag between displacer motion and pressure in the expansion chamber, the expanding gas performs mechanical work on the displacer, thus producing cooling effect. During the expansion stage of a thermodynamic cycle, the heat is absorbed from the cold finger tip; during the successive compression stage the heat is rejected at the warm side, as detailed, for example, in [1].

A force couple generated by imbalanced reciprocation of moving components inside both compressor and expander result in cryocooler induced vibration comprising angular and translational tonal components. High resolution, long range IR imagers are usually sensitive to the line of sight jitter and/or dynamic defocusing resulting from cryocooler induced vibration. Improving imagery quality requires, therefore, attenuating this vibration down to the acceptable levels.

Typical of such cryogenic coolers is a linear, almost sinusoidal, reciprocation of the moving piston and displacer assemblies. The temperature control relies on varying the magnitude of the driving voltage at a fixed driving frequency.

This results in the axial, almost tonal vibration export, the frequency of which is fixed and magnitude of which varies depending on the heat load conditions. The driving frequency may be precisely (factory or user) adjusted and maintained over the range of working conditions and lifetime using a digital controller. Setting the driving frequency over the range ±2Hz about optimum frequency is practically not affecting the cryocooler performance.
Because of the fixed and adjustable driving frequency, the low damped tuned dynamic absorber (TDA) appears to be ideally suited and cost effective~~,~~lightweight tool for attenuation of cooler induced vibration, thus improving optical performance of such inherently vibration sensitive IR imagers. It is usually designed in the form of passive and weakly damped mass-spring resonator attached to a dynamic structure subjected to a tonal excitation. Provided resonant frequency of TDA and frequency of excitation are precisely matched, such a device produces a tonal counterbalancing dynamic reaction, thus eventually attenuating the dynamic response of the attachment point, as detailed in references [2-9].
In the recent years, manufacturers of low SWAP (Size, Weight and Power) split Stirling linear cryocoolers and Integrated Dewar Detector Cooler Assemblies (IDDCA), such as Ricor, AIM and SCD [10-21] developed and fielded new models of optional TDA intended for use in vibration sensitive lightweight and flexibly mounted, hand-held and gyro-stabilized payloads relying on cost effective split Stirling cryogenic coolers featuring single piston compressors. Known are also examples of cryogenically cooled long-range thermal weapon sights (TWS), relying on the optional TDA [22,23].
Usually, such a TDA is made in the form of an undamped "mass-spring" single degree of freedom (SDOF) translational system, where the frequencies of "parasitic" modes (tilting, in-plane translations, rotation about the axis" are well separated from the frequency of axial translational mode, the frequency of which needs to be tuned exactly to the driving frequency (or vice versa).
Although the vibration export produced by the expander is relatively weak, it cannot be disregarded in the modern light-weight hand held and gyrostabilized electro-optic applications. In these cases, it is strongly recommended to in-line mount of compressor and expander. Single-axis consolidation of vibration export induced by compressor and expander allows for effective use of single, inline mounted translational TDA [20,21], as shown in Figure 1.

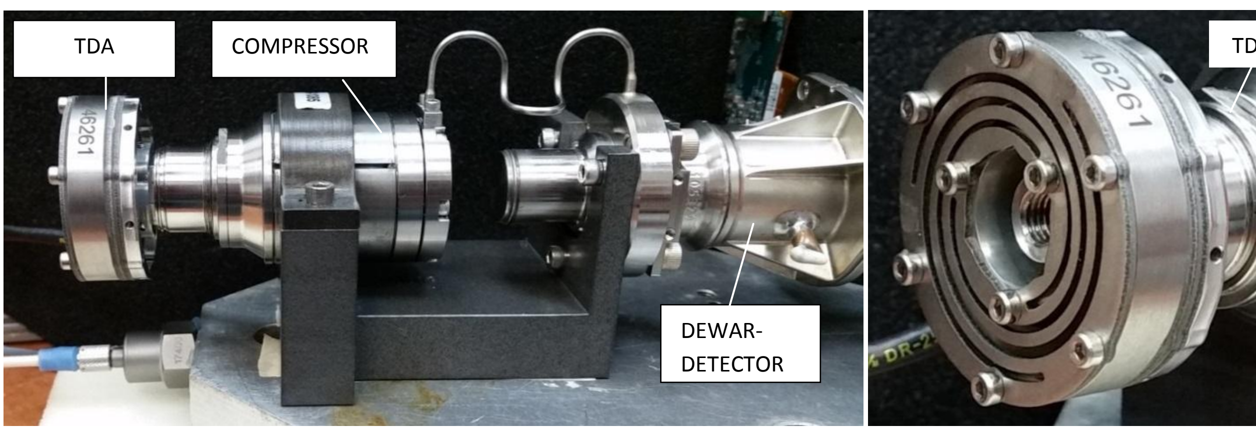

Figure 1. SDOF tuned dynamic absorber in application to vibration attenuation of inline split Stirling linear cryogenic cooler (Ricor model K527)

Unfortunately, this option is not always practical due to the different packaging constrains. For compactness, the expander and compressor may be side-by-side packaged. In this approach, expander-induced vibration export may produce moment about the payload center of gravity resulting in angular line-of-sight jitter along with translational defocusing. In this case, two matched TDA may be used. The obvious penalties are: added weight, size and frequency matching complexity.
The authors are continuing exploring the concept of Multimodal Tuned Dynamic Absorber (MTDA) – undamped mechanical resonator featuring a plurality of useful dynamic modes, the frequencies of which are essentially matched with the driving frequency. The general idea lying behind this concept is that such a device may produce reactions (forces and moments) counterbalancing complex vibrational export produced by a component of split Stirling cryogencic cooler. In this paper they will consider two types of such devices: cantilever dynamic absorber featuring matched bending and torsion modes and circular dynamic absorber featuring matched translational and angular modes

[24-25]. For the better informativeness of the presentation, the Finite Elements (FE) technique will be used. The outcomes on numerical simulation are supported by full scale experimentation.

2. CANTILEVER TUNED DYNAMIC ABSORBER

The dynamic system in Figure 2 consists of the cantilever round bar of circular cross-section carrying thin disk at its tip. The rod is characterized by diameter d and length L; the Young and shear modules are E and $G = 0.5E/(1+\mu)$, respectively, where μ is the Poisson ratio; cross sectional and polar moments of inertia are $J_1 = \pi d^4/64$ and $J_2 = \pi d^3/32$, respectively. The disk has radius R and mass M. The moment of inertia of disk about its central axis and about its in plane central axis are $I_1 = 0.25MR^2$ and $I_2 = 0.5MR^2$, respectively.

For the first bending mode, using Dunkerley formula [26] and neglecting the bar weight, the approximate expression for the resonant frequency is

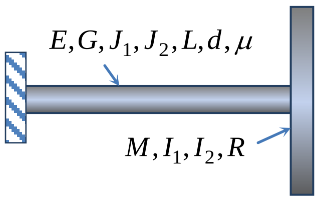

Figure 2. Dynamic model

$$\Omega_b^2 \approx \frac{3EJ_1}{L^3\left(M + \frac{3I_1}{L^2}\right)} = \frac{3E\frac{\pi}{64}d^4}{ML\left(L^2 + \frac{3}{4}R^2\right)} \tag{1}$$

Along with these lines, for the torsional mode, the expression for the resonant frequency is

$$\Omega_t^2 = \frac{GJ_2}{LI_2} = \frac{E\frac{\pi}{32}d^4}{2(1+\mu)L\frac{1}{2}MR^2} = \frac{E\frac{\pi}{32}d^4}{(1+\mu)LMR^2} \tag{2}$$

From (1) and (2), the frequencies of bending and torsion may be equalized when

$$L \approx R\sqrt{0.75 + 1.5\mu} \tag{3}$$

It is worth noting that, in this particular case the optimal position of disk depends on its radius and Poisson ratio only. The value of the resonant frequency may be "tuned" conveniently by choosing appropriate diameter, d, of the bar. Simple condition (3) will be used below as initial guess in FE assisted design. Different shapes of the disks are also possible.

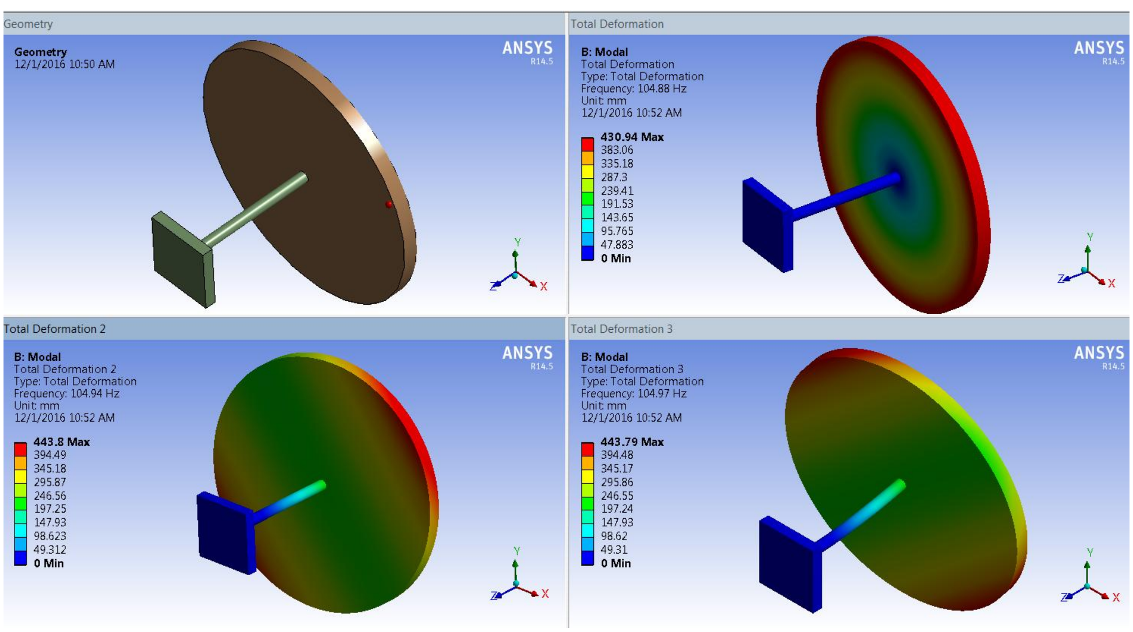

Figure 3. Modal analysis

In this exemplary design, the MTDA features Ti-4V-6Al-ELI (Grade 23) cantilever rod of diameter 1*mm* and active length $L = 12.63mm$ along with W90Cu10 disk of diameter 23.6*mm* and thickness 1.35*mm*. The bending and torsional modes of this MTDA are tuned to have frequencies about 104.9Hz (see results of FE modal analysis in Figure 3). The total weight of MTDA is 22 g (3.7% of the total module weight). Tuning procedure of such a MTDA involves displacing of the disk along the rod length and monitoring the bending and torsional frequencies.

It is worth noting that for this material having typical Poisson ratio $\mu = 0.28$, formula (3) yields $L = 12.76mm$. Figure 4.a shows the cryogenic module where compressor and cold head are in plane side-by-side packed for the sake of compactness. The dynamic system considered above may be used as MTDA featuring matched bending and torsional modes, as shown in Figure 4.b, where the MTDA is mounted upon the compressor.

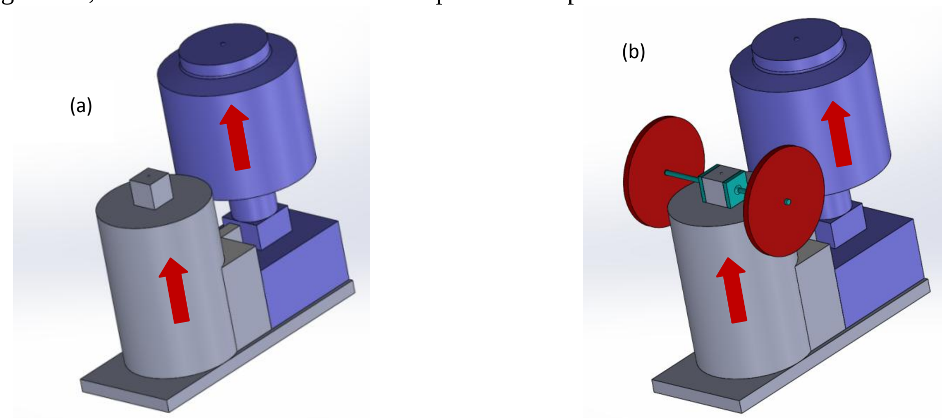

Figure 4. Side by side packaged split Stirling cryogenic cooler with no and with cantilever tuned dynamic absorber

The magnitudes of these forces equal the product of moving mass, stroke and driving frequency squared, as explained in [26]. There also exists a particular phase lag between these two forces. Further, in this particular study, the compressor and expander vibration export will be 8N@105Hz and 3N@105Hz, respectively. Without loss of generality, the phase lag is assumed to be 90deg.

For the purpose of FE analysis, the cryocooler base has been suspended from the stationary base by the weak springs mimicking low frequency vibration mount featuring frequencies well below the driving frequency. Figure 5 shows the simulated translational (***X*** and ***Z***) and angular (***Φ***) frequency responses of cryogenic module measured at the location of cold finger tip over the range 100-110Hz with and without MTDA. In all the simulations we assume the damping ratio of MTDA to be as low as 0.02%.

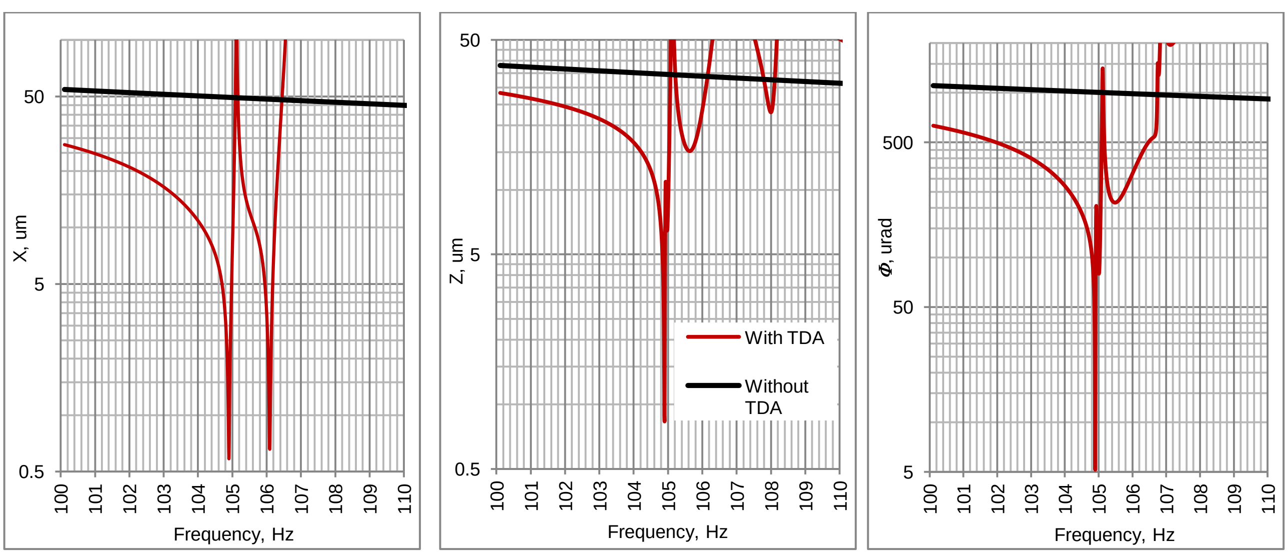

(a) (b) (c)

Figure 5. Dynamic responses of cryomodule without and with MTDA

From Figure 5, the simulated frequency responses of the cryogenic module equipped with MTDA feature deep antiresonant notches at the frequency 104.9Hz followed by the high frequency resonances. Figure 6 shows the outcomes of FE simulation at the frequency 104.9Hz: dynamic deflection in ZX plane of the cryogenic module without MTDA (weak springs not shown). From Figure 6.a, without MTDA the cryomodule is involved in complex motion comprising both translational and angular components. In Figures 6.b,c, the cryogenic module is practically stationary while the MTDA masses are involved in intensive vibration comprising both angular and bending components.

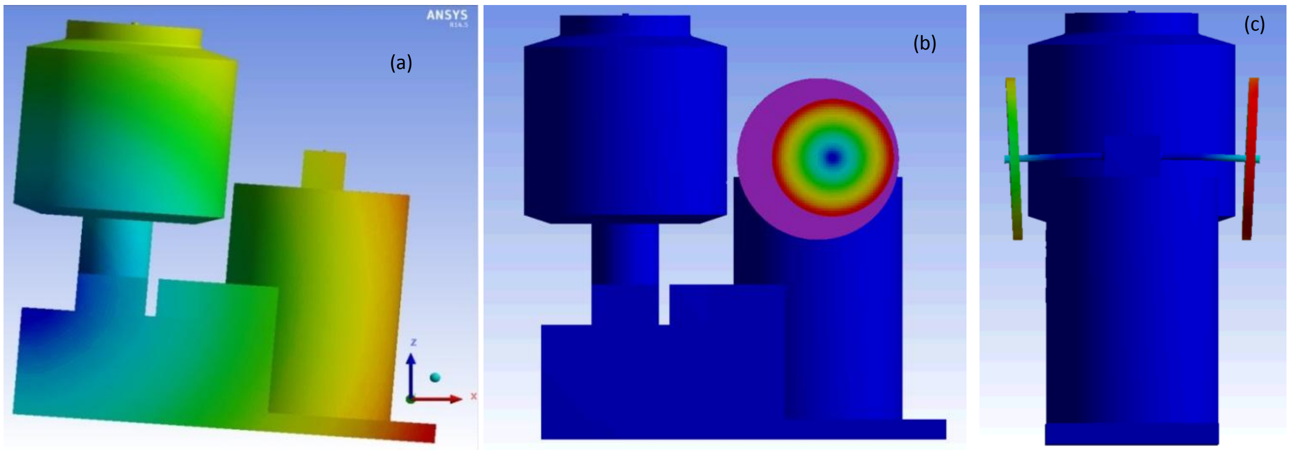

Figure 6. Dynamic responses of cryomodule without and with MTDA

For the sake of design compactness, the thin discs may be substituted by solid cylinders of smaller diameter. Figure 7.a shows the spring comprising two round flexure beams symmetrically extending from the common base and featuring threaded ends for mounting cylindrical bodies, as portrayed in Figure 17.b.

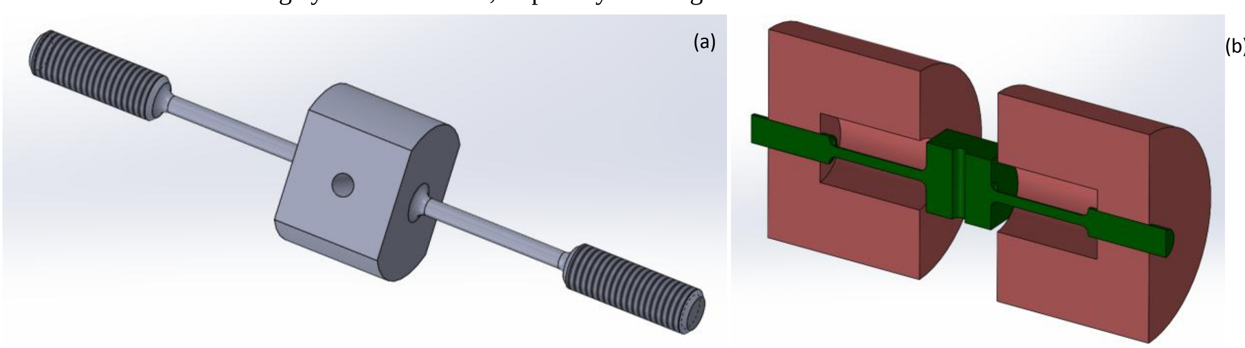

Figure 7. Dynamic system

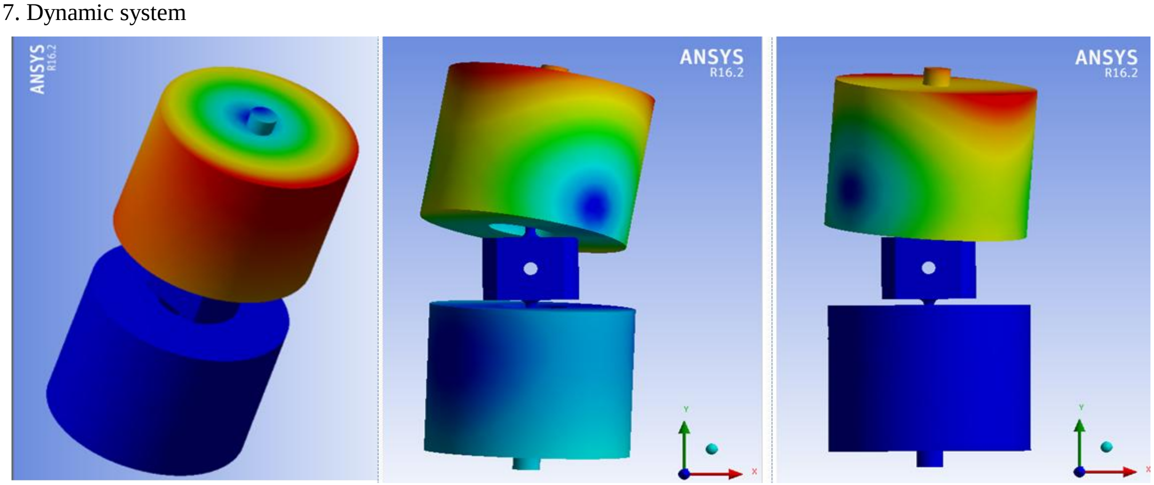

Figure 8. Modal analysis

The frequencies of bending and torsional modes were equalized by displacing proof bodies along the beams. In this exemplary design, the Ti-4V-6Al-ELI beams were considered along with W90Cu10 proof masses. Figure 8 shows the 3 relevant torsional and bending modes tuned to 105Hz.
Figure 9 shows the cryogenic module where compressor and cold head are in plane side-by-side packed without (a) and with MTDA (b).

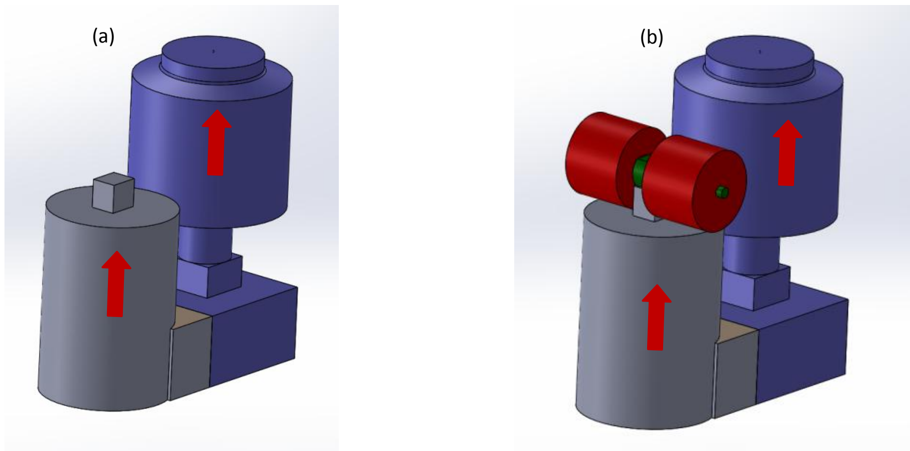

Figure 9. In-plane side-by-side packed cryogenic module without (a) and with MTDA (b).

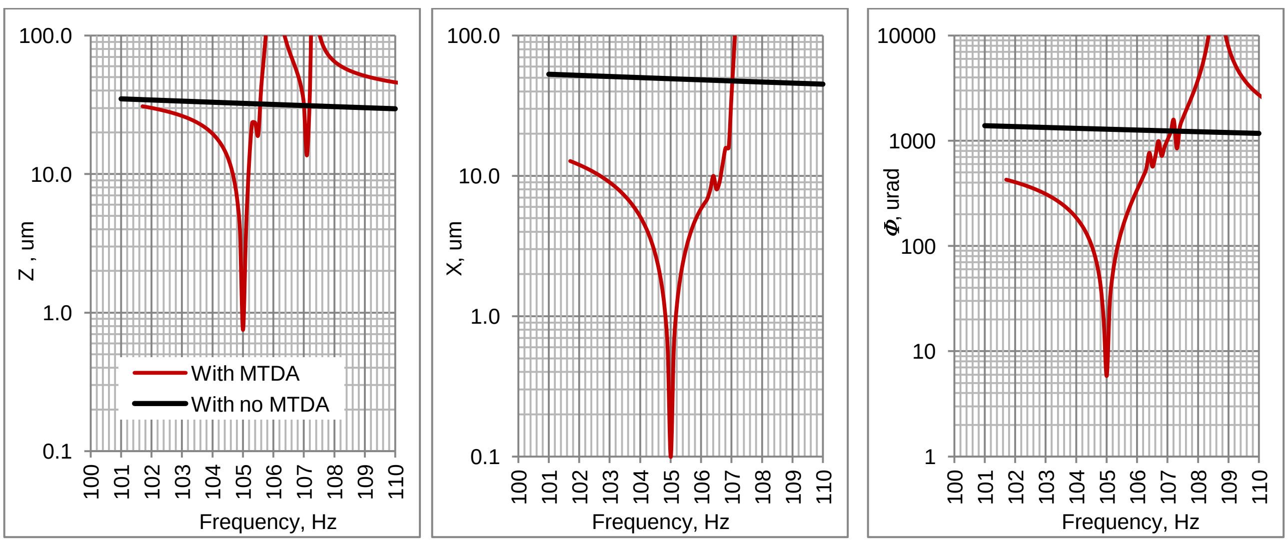

(a) (b) (c)

Figure 10. Dynamic responses of cryomodule without and with MTDA

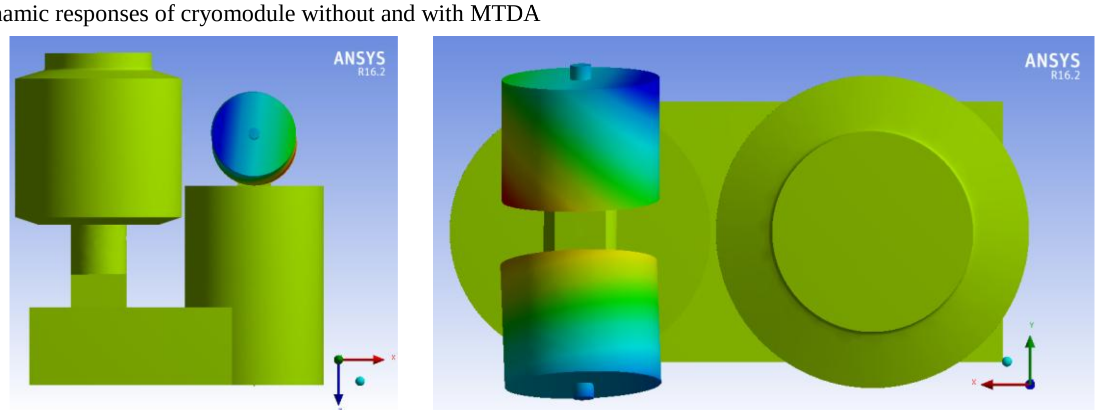

Figure 11. Dynamic response of cryomodule with MTDA

Figure 10 shows the simulated translational (***X*** and ***Z***) and angular (***Φ***) frequency responses of cryogenic module measured at the location of cold finger tip over the range 100-110Hz with and without MTDA. In all the simulations we assume the damping ratio of MTDA to be as low as 0.02%.
Figure 11 shows the outcomes of FE simulation at the frequency 105Hz: dynamic deflection in ZX plane of the cryogenic module with MTDA (weak springs not shown). As different from the reference Figure 6.a, the cryogenic module is practically stationary while the MTDA masses are involved in intensive vibration comprising both angular and bending components.

3. CIRCULAR MULTIMODAL TUNED DYNAMIC ABSORBER

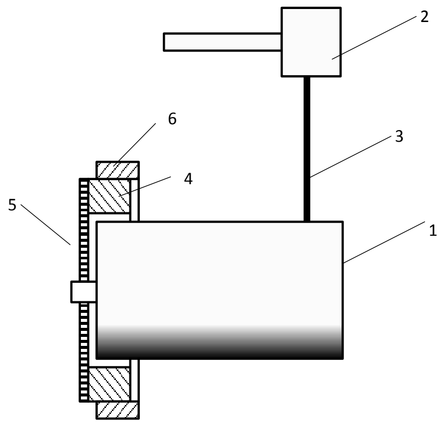

Figure 12. Side-by-side packed split Stirling cryogenic cooler with circular MTDA

Different design embodiment describes patent pending circular MTDA [24,25] for using with in plane side-by-side packed split Stirling cryogenic cooler. Figure 12 shows diagrammatic view of the side-by-side packed split Stirling cryogenic cooler comprised of compressor 1 and expander 2 interconnected by the transfer line 3, whereupon the circular MTDA includes primary proof ring 4 which is supported from one side by the flexural bearing 5 having central anchor for mounting to compressor housing 1. The secondary proof ring 6 is coaxial and displaceable along the primary proof ring. In this embodiment, the flexural bearing is made in the form of a circular planar spring with 4 symmetrical spiral slots. The frequencies of translational and two tilting modes of such an MTDA are essentially tuned to the driving frequency.
In this embodiment, the translational frequency depends on the weight of the aggregate body and axial spring rate of the flexural bearing. Along with these lines, the tilting frequencies depend on the angular spring rate of the flexural bearing and aggregate moment of inertia of the rings. By mechanical design of the flexural bearing and rings, the frequencies of the translation and tilting modes may be equalized and made essentially equal the fixed working frequency typical of the cryocooler. Fine tuning may be performed by axially displacing the secondary ring, thus modifying the tilting frequency at fixed translational frequency, as detailed in [24,25].
Figure 13 shows the flexural bearing (a) and self-explanatory exploded view (b) of actual CAD design of such a MTDA.

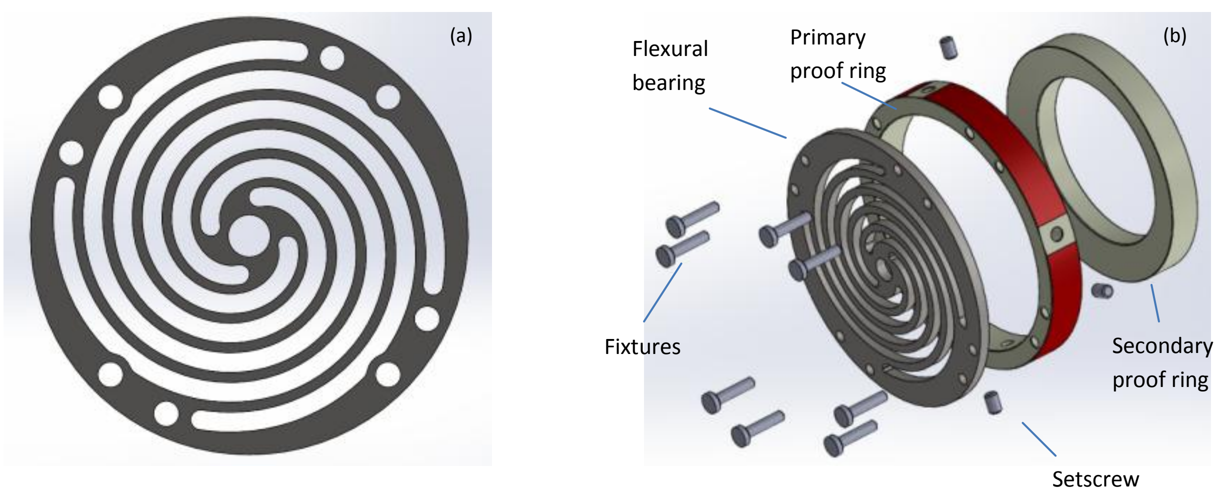

Figure 13. Design of circular MTDA

Figure 14 shows the first 6 modal shapes: rotation about MTDA axis (a), translation along the MTDA axis (b), tilting modes (c,d) and in plane modes (e,f). The frequencies of tilting and translation modes are 105Hz. This has been achieved by virtually displacing the correction ring into particular position, it will be loosely set to “zero”. The frequency of rotational mode is 65Hz, the frequencies of the in plane modes are 195Hz.

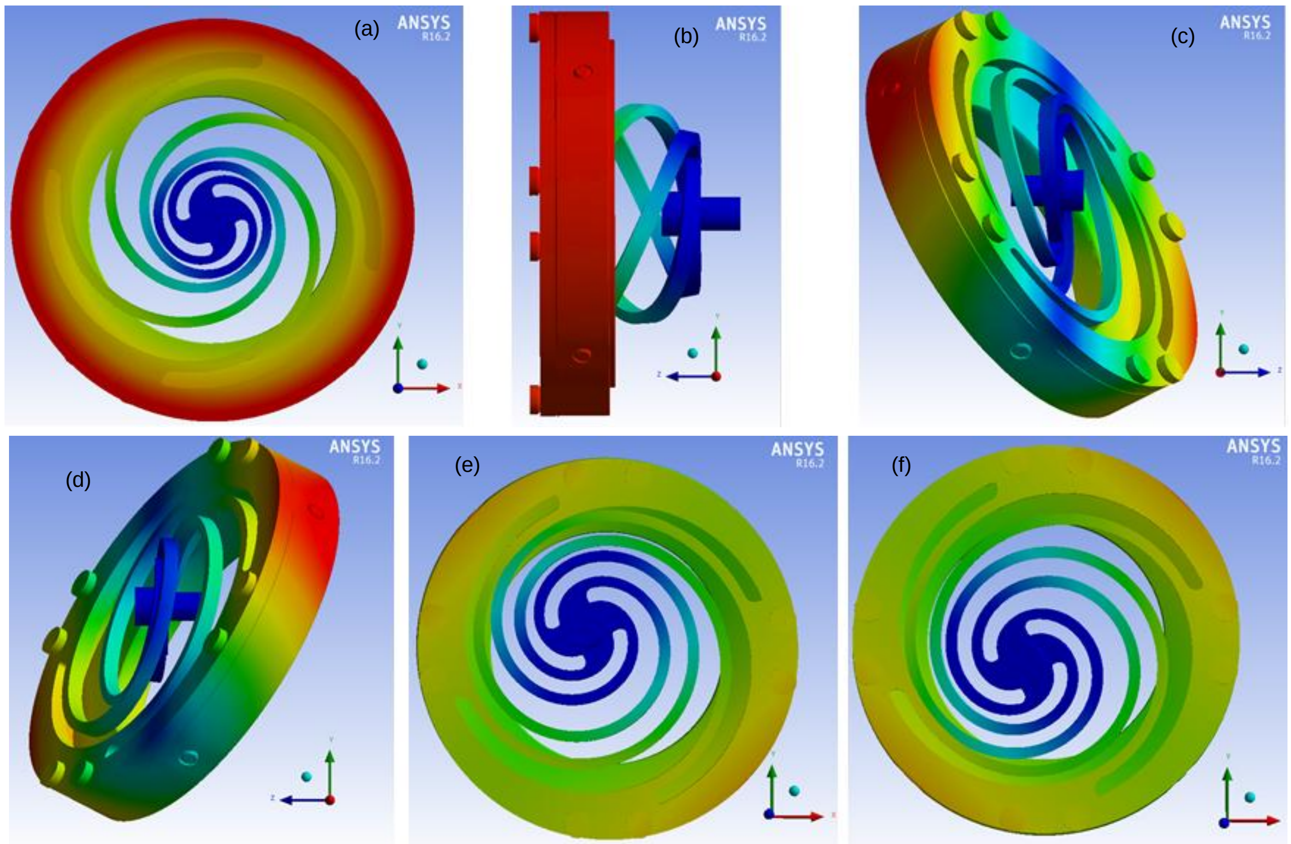

Figure 14. Dynamic modes

Figure 15 shows the model of in plane side-by-side packed split Stirling cryocooler with mounted MTDA. In Figure 15, the MTDA axis is collinear with the compressor and cold head axes. The red arrows show the direction of applied forces, 8N@105Hz along the compressor axis and 3N@105Hz along the cold head axis. The weak springs are nor shown.

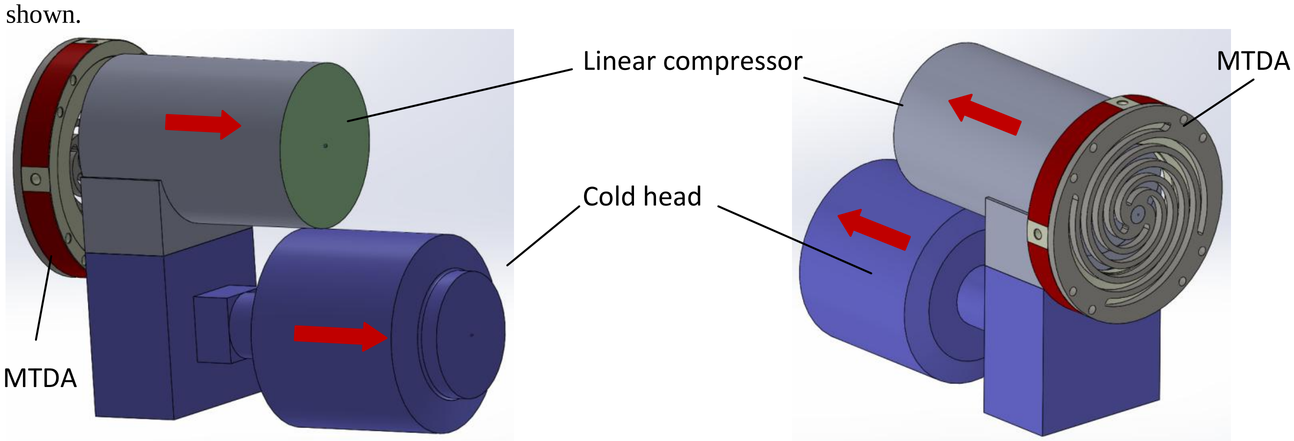

Figure 15. In-plane side-by-side packed cryogenic module with MTDA.

Figure 16 shows the simulated translational (***X*** and ***Z***) and angular (***Φ***) frequency responses of cryogenic module measured at the location of cold finger tip over the range 100-110Hz with and without MTDA. In all the simulations we assume the damping ratio of MTDA to be as low as 0.02%.

Figure 17 shows the outcomes of FE simulation at the frequency 105Hz: dynamic deflection in ZX plane of the cryogenic module without MTDA (a) and with MTDA (b). From Figures 17 with no MTDA the cryomodule is involved in complex motion comprising translational and angular components; with MTDA the cryogenic module is practically stationary while the MTDA mass are involved in intensive, both translational and angular vibration.

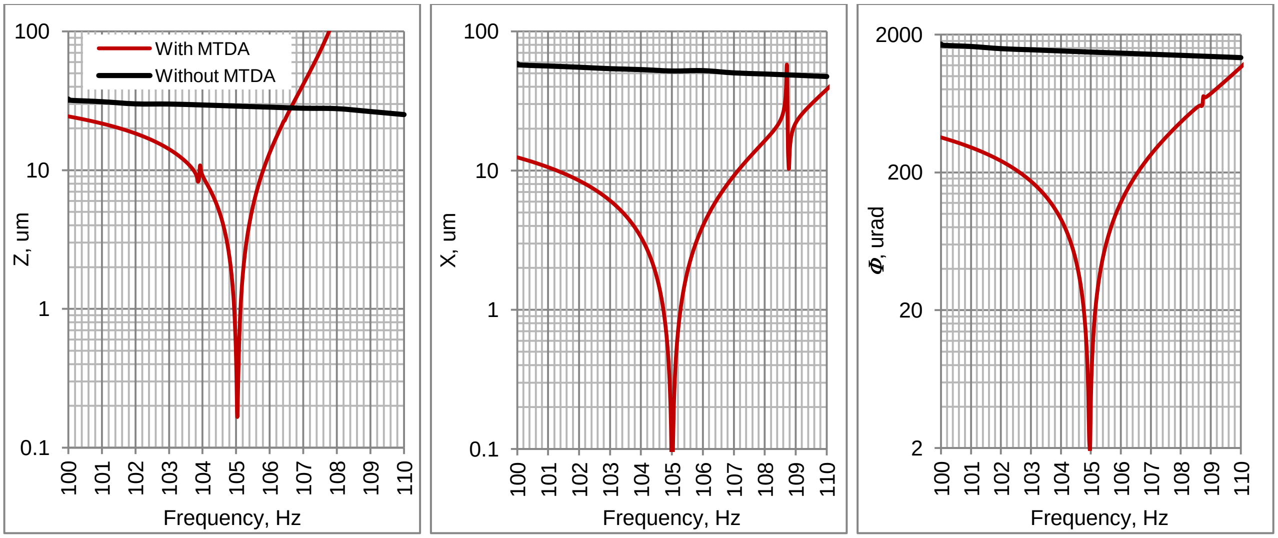

(a) (b) (c)

Figure 16 . Dynamic responses of cryomodule with and without MTDA

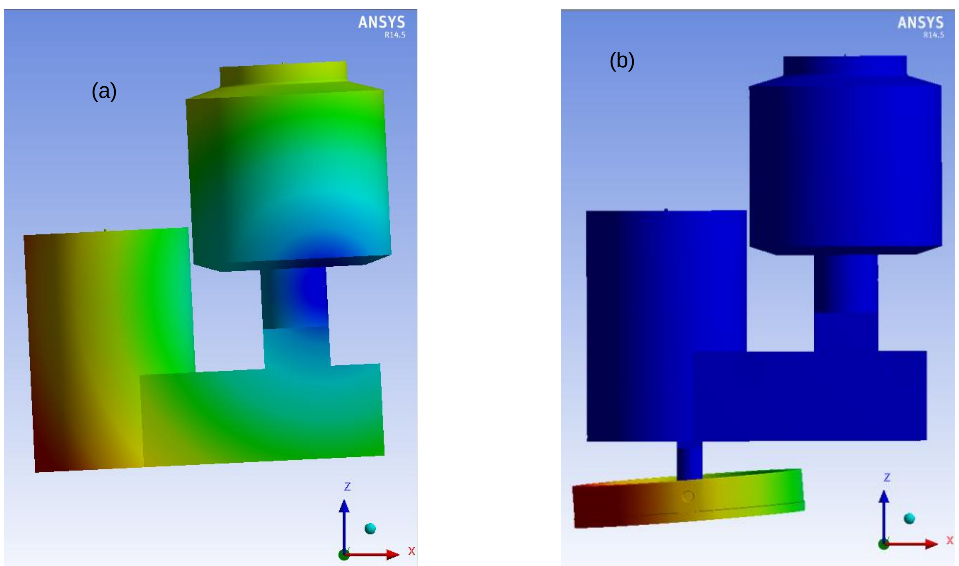

Figure 17. Dynamic response of cryomodule without (a) and with MTDA (b)

4. FEASIBILITY STUDY

Figure 18 shows the experimental setup. The miniature electrodynamic vibration exciter 1 is fixedly clamped at the top of vibration mounted platform 2 weighting approximately 2 kg. Two studs 3 and 4 are mounted upon the platform in line with the exciter and allow for mounting dynamic absorbers with different offsets relative to the exciter axis. Figure 19 shows variants of mounting of the cantilever MTDAs (a,b), and circular MTDA (c).

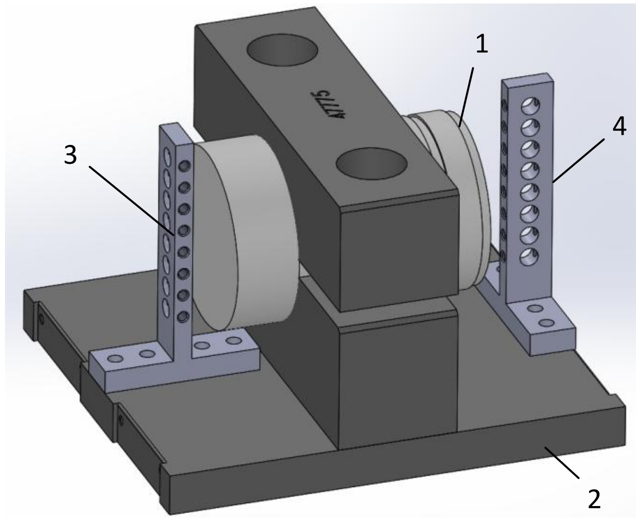

Figure 18. Experimental setup

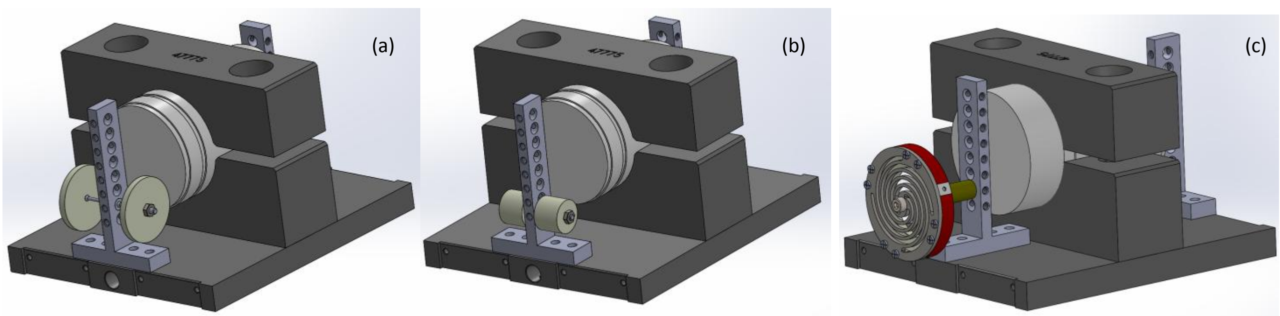

Figure 19. Testing different MTDAs

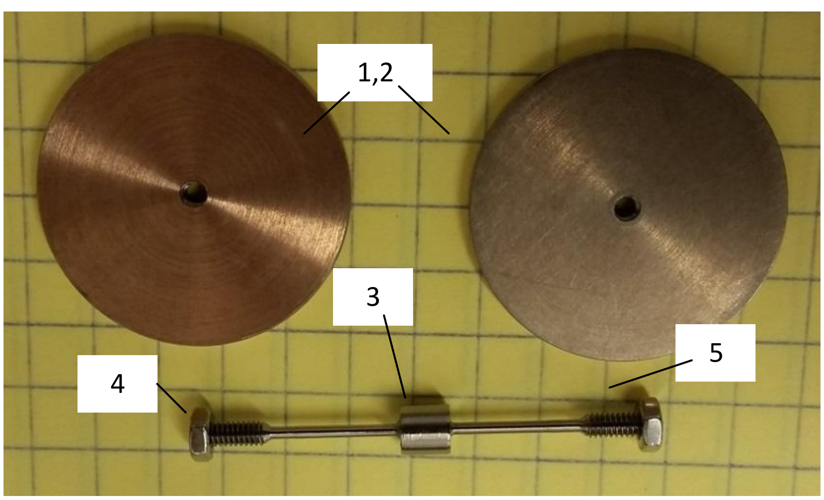

Figure 20 . Enhanced planar omnidirectional MTDA

4.1. Cantilever multimodal tuned dynamic absorber (Type 1)

Figure 20 (grid size is 5mm) shows the first embodiment of enhanced planar omnidirectional MTDA, comprising two proof weights made in the form of centrally threaded thin discs 1,2 made of heavy alloy W90Cu10 and Ti-6Al-4V-ELI spring 3 featuring central anchoring feature along with two threaded ends.

The effective weight of MTDA is 30 grams. Fine frequency tuning is achieved by rotating discs until reaching best vibration attenuation performance at the prescribed frequency. Two nuts 4,5 are used for locking discs positions. Because of the manufacturing tolerances and possible discrepancies in mechanical properties, the best performance may be achieved at a frequency which is slightly different from the theoretical prediction. This is quite acceptable in case of linear cryocooler, the driving frequency of which may be precisely adjusted over a range of ±2Hz about the optimal driving frequency without affecting its thermomechanical performance.

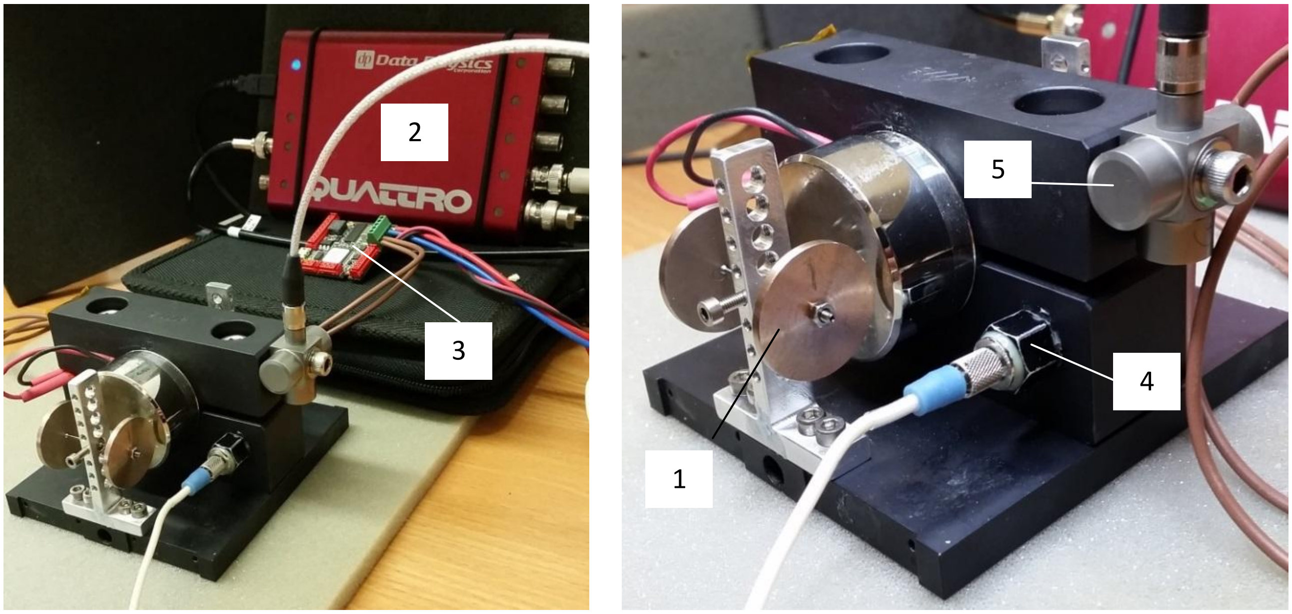

Figure 21. Experimental setup

Figure 21 shows the experimental setup, where the MTTDA 1 is mounted with 5 mm offset relatively to the exciter axis. The driving tonal signal is generated by the Data Physics SignalCalc QUATTRO signal analyzer (see http://www.dataphysics.com) 2 and amplified by the Ingenia Neptune digital servo drive 3 (see www.ingeniamc.com). The Endevko Type 256HX-10 accelerometer 4 is used for measuring resulting translational response. The Kistler Type 8838 accelerometer (see https://www.kistler.com) 5 is mounted upon the platform and is used for measuring resulting angular response. The effective weight of the setup is about 2kg, thus the mass ratio is 1.5%. The entire setup is placed upon soft sponge mimicking conditions typical for the hand-held applications or low frequency vibration mounting.

Figure 22 compares spectra of translational (a) and angular acceleration (b), respectively, of the platform before and after mounting the MTDA. Simultaneous attenuation of angular and translational responses occurred at approximately 103Hz, whereupon the translational and angular attenuation ratios are 40 and 44, respectively. From Figure 29, the translational and angular displacement of the platform has been reduced from 4.8 μm to 0.11 μm and from 54 μrad down to 1.2 μrad, respectively. It is worth noting that attenuation of the angular response resulting in a line of sight jitter is more important for the imagery quality.

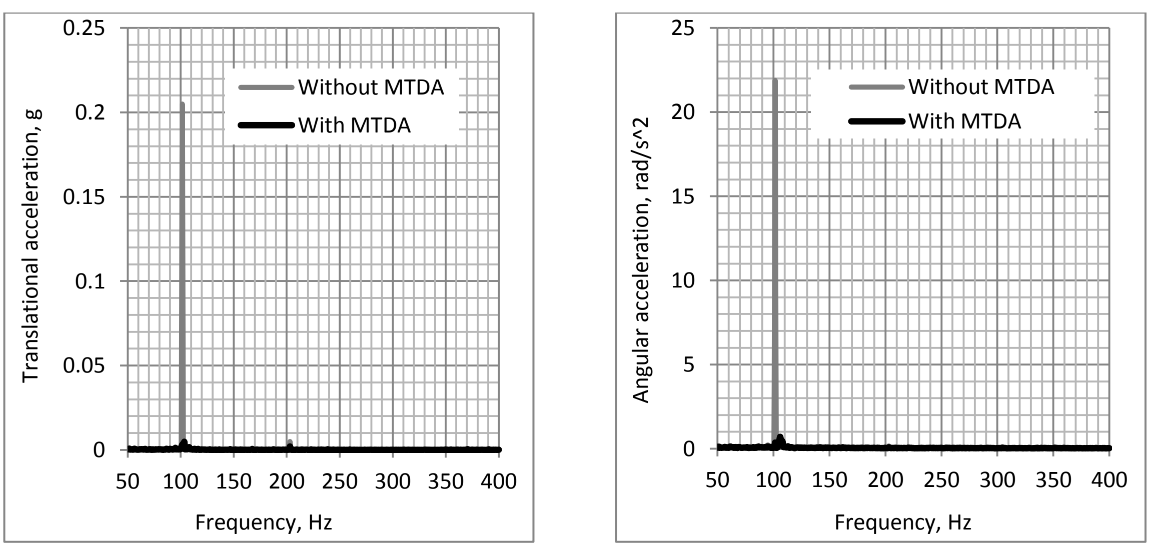

(a) (b)

Figure 22. Spectra of translational and angular accelerations of platform with and without MTDA

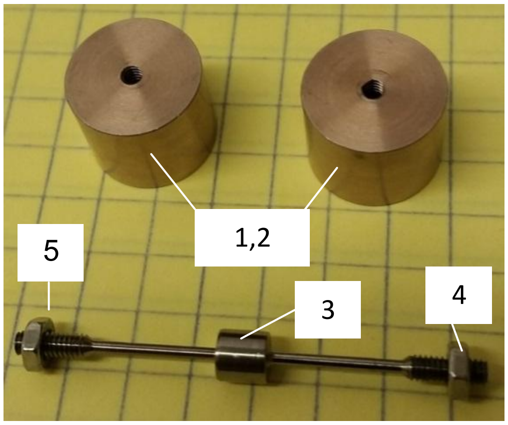

Figure 23. Enhanced planar omnidirectional MTDA

4.2 Cantilever multimodal tuned dynamic absorber (Type 2)

Figure 23 (grid size is 5mm) shows another embodiment of cantilever MTDA, comprising two centrally threaded proof weights 1,2 made of above mentioned heavy alloy W90Cu10 and Ti-6Al-4V-ELI spring 3 featuring central anchoring feature and two threaded ends. The effective weight of MTDA is 30 grams. Fine frequency tuning is achieved by rotating cylinders until reaching best vibration attenuation performance. Two nuts 4,5 are used for locking proof weights positions.

Figure 24 shows the experimental setup, where the MTTDA is mounted with 5 mm offset relatively to the exciter axis. The rest of notations are as in Figure 21. Figure 25 compares spectra of translational (a) and angular acceleration (b), respectively, of the platform before and after mounting the MTDA.

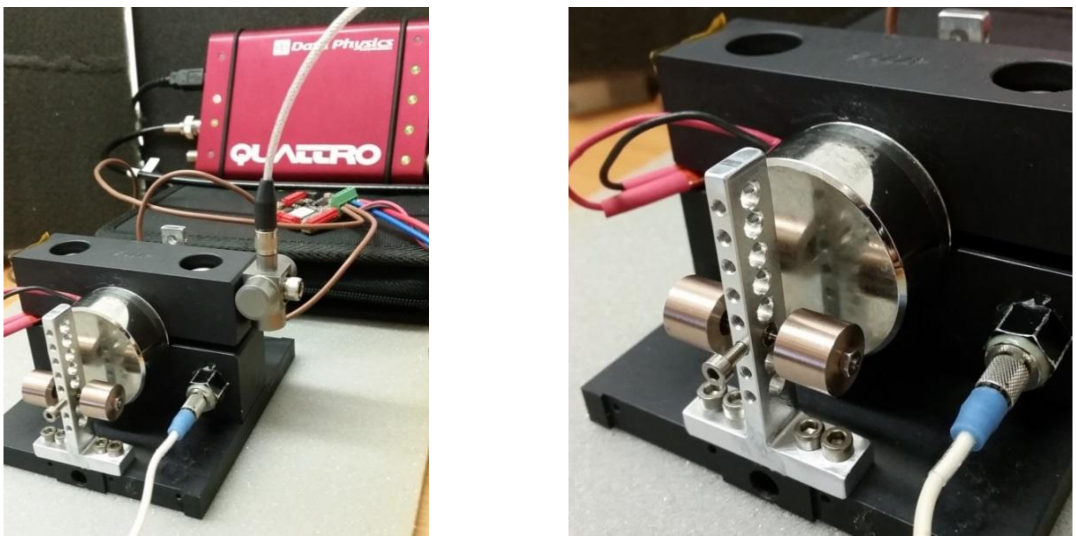

Figure 24. Experimental setup

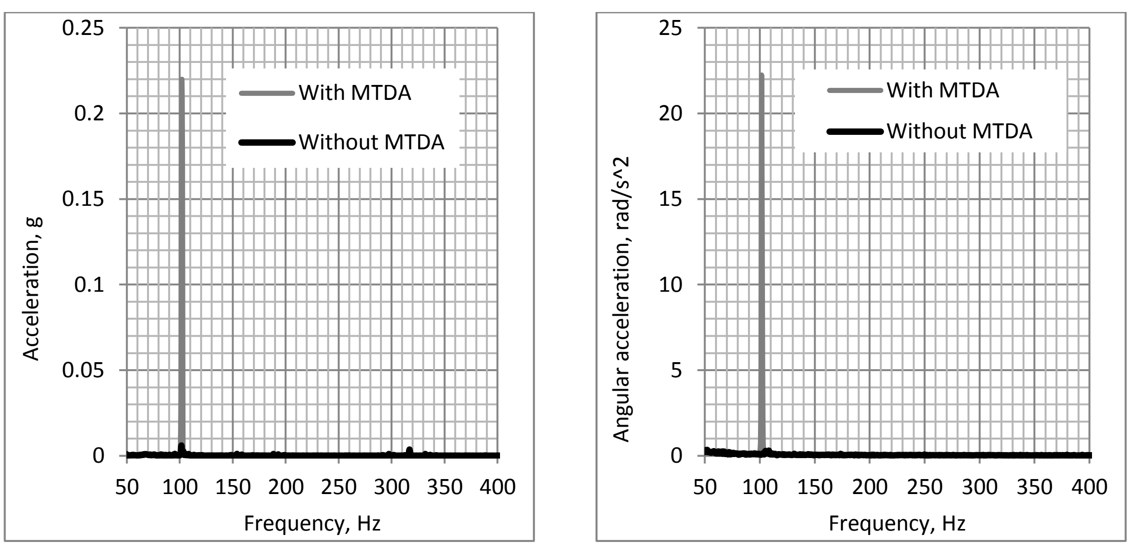

(a) (b)

Figure 25. Spectra of translational and angular accelerations of platform with and without MTDA

4.3. Circular multimodal tuned dynamic absorber

Figure 26 pictures the assembled circular MTDA (a) comprising flexural bearing (b), primary ring with mounted flexural bearing (c) and secondary corrective proof ring (d).

(a)

(b)

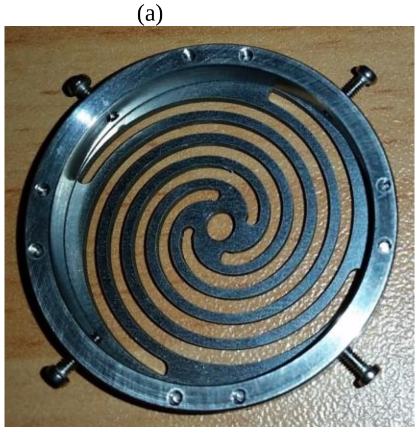

(c)

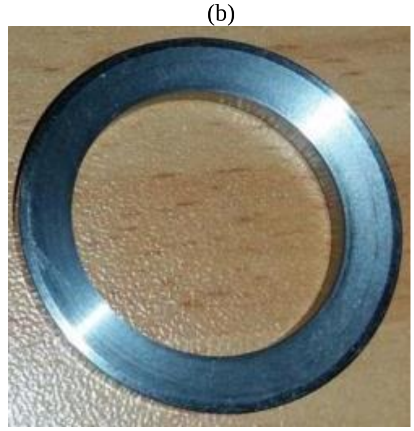

(d)

Figure 26. Circular MTDA parts and assembly

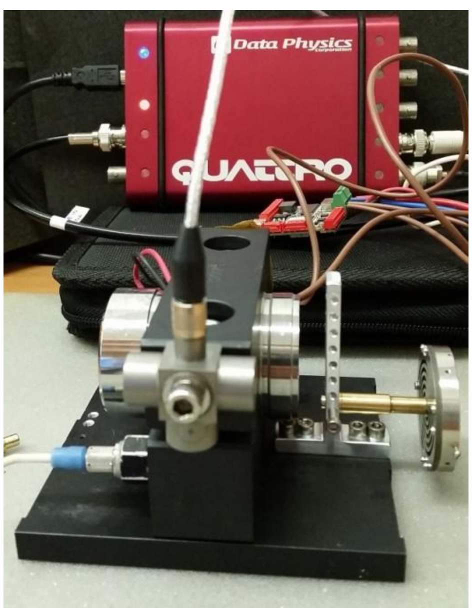

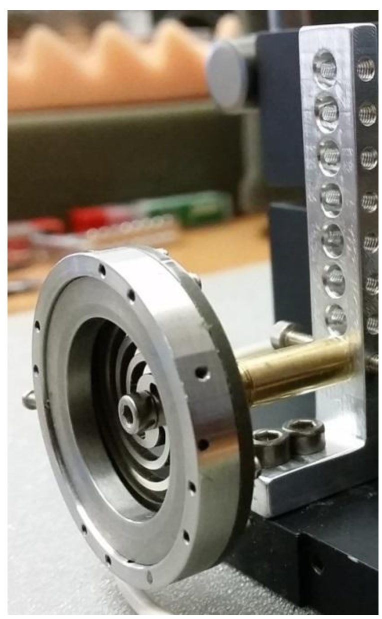

Figure 27. Experimental setup

Figure 27 shows the experimental setup, where the circular MTTDA is mounted with 20 mm offset relatively to the exciter axis. The rest of notations are as in Figure 21. The frequency match has been achieved by axial displacing the secondary corrective ring.

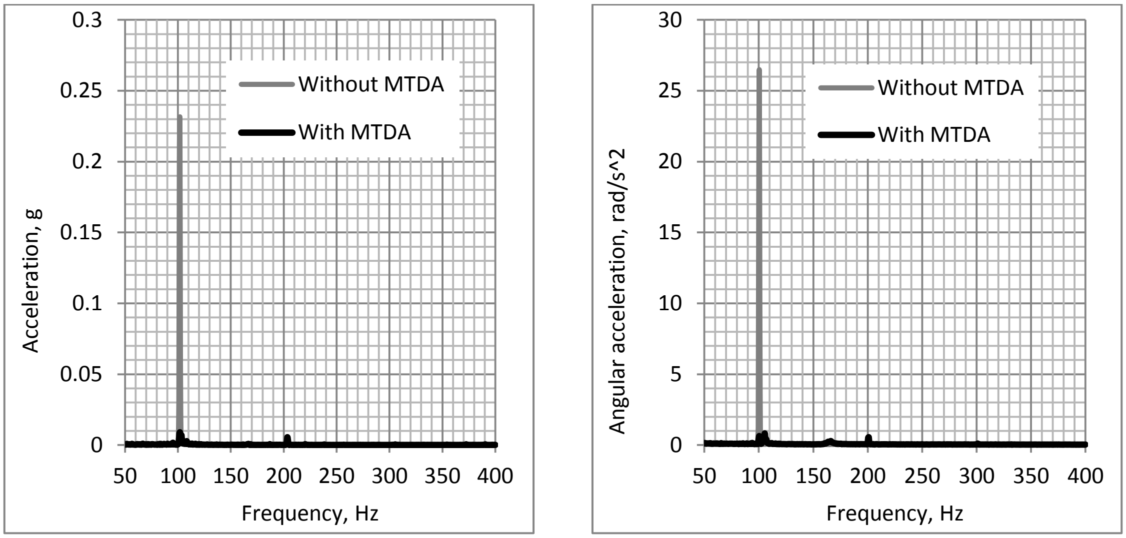

(a) (b)

Figure 28. Spectra of translational and angular accelerations of platform with and without MTDA

Figure 28 compares spectra of translational (a) and angular acceleration (b), respectively, of the platform before and after mounting the MTDA. Simultaneous attenuation of angular and translational responses occurred at approximately 103Hz, whereupon the translational and angular attenuation ratios are 33 and 52, respectively. From Figure 28, the translational and angular displacement of the platform has been reduced from 5.4 μm to 0.16 μm and from 63 μrad down to 1.2 μrad, respectively. It is worth noting again that attenuation of the angular response resulting in a line of sight jitter is more important for the imagery quality.

CONCLUSIONS AND FUTUTRE WORK

The analytical study and full scale feasibility testing has shown that multimodal tuned dynamic absorbers have improved potential for essential attenuation of line of sight jitter resulting from the cryocooler induced angular vibration.
At the same time, the tuning procedure is much more complicated as compared with the case of traditional single degree of freedom tuned dynamic absorber. There is a need, therefore, in development different embodiments allowing for more convenient tuning procedures

ACKNOLEDGEMENTS

The authors are thankful to Mr Eli Steinitz for the technical support.

REFERENCES

[1] Walker G , [Cryogenic coolers, Part 2 – Applications], Plenum Press, New York, (1983).
[2] Ormondroyd J., and Den Hartog J.P., "The theory of the dynamic vibration absorber", Transactions of ASME 50, (1928).
[3] Brock, J. E., "A Note on the Damped Vibration Absorber", J. Appl. Mech., 13 p. A284, (1946).
[4] Snowdon J.C., [Vibration and shock in damped mechanical systems], John Wiley, NY, (1968).
[5] [Harris' Shock and Vibration Handbook], Sixth Edition, McGraw-Hill: New York, (2010)
[6] Timoshenko, S., Young, D. H. and Weaver, W. Jr., [Vibration Problems in Engineering], Edition 4th ed., New York, Wiley, (1974)
[7] Den Hartog, J. P., [Mechanical Vibrations], 4th ed., Dover Publications, New York, (1985).

[8] Inman, D. J., Singh, R.C., [Engineering vibration], Prentice Hall Upper Saddle River, (2001)
[9] Thompson A.G., "Optimum tuning and damping of a dynamic vibration absorber applied to a force excited and damped primary system", Journal of Sound and Vibration, Volume 77, Issue 3, 403-415, (1981).
[10] Veprik, A., Babitsky, V., Pundak, N. and Riabzev, S., "Vibration control of linear split Stirling cryogenic cooler for airborne infrared application", Shock and Vibration, 7 (6), 363-379 (2000)
[11] Veprik, A., Vilenchik, H., Pundak, N., "Microminiature linear split Stirling cryogenic cooler for portable infrared imagers", Proc. Cryocoolers 14, 105-115 (2006).
[12] Veprik, A., Vilenchik, H., Riabzev, S., Pundak, N., "Novel microminiature linear split Stirling cryogenic cooler for portable infrared imagers", Proc. SPIE, 6542, 65422F (2007).
[13] Veprik, A., Zechtzer, S. and Pundak N., "Compact linear split Stirling cryogenic cooler for high temperature infrared imagers", Proc. Cryocoolers 16, 121-132 (2008).
[14] Veprik, A., Zechtzer, S. and Pundak N., "Split Stirling linear cryogenic cooler for a new generation of high temperature infrared imagers", Proc. SPIE 7660, 76602K (2010).
[15] Veprik, A., Zechtzer, S., Pundak, N., Kirkconnell, C., Freeman, J. and Riabzev, S., "Adaptation of the low cost and low power tactical split Stirling cryogenic cooler for aerospace applications", Proc. SPIE 8012, 80122J (2011)
[16] Veprik A., Riabzev, S., Avishay, N., Oster, D., and Tuitto, A., "Linear cryogenic coolers for HOT infrared detectors", Proc. SPIE. 8353, 83531V (2012).
[17] Rühlich, I., Mai, M., Rosenhagen, C. et al., "Compact high-efficiency linear cryocooler in single-piston moving magnet design for HOT detectors", Proc. SPIE 8353, 83531T (2012).
[18] Rühlich, I., Mai, M., Withopf, A. et al., "AIM cryocooler developments for HOT detectors", Proc. SPIE 9070, 90702P (2014).
[19] Rosenhagen, C. and Rühlich, I., "Compensating oscillation device", European Patent WO 2014206542 A1 (2014)
[20] Veprik, A., Tuitto, A., “Tuned dynamic absorber for split Stirling cryogenic cooler”, Proc. SPIE. 9821, Tri-Technology Device Refrigeration (TTDR), 98210F (2016).
[21] Veprik, A., Babitsky, V., “Ultra-light weight undamped tuned dynamic absorber for cryogenically cooled infrared electro-optic payload”, Cryogenics, 83, pp 22-30 (2017)
[22] http://www.aim-ir.com/fileadmin/files/Data_Sheets_Thermal_sights/2013_neu/2013_AIM_datenblatt_A4_HuntIR-K2_engl.pdf
[23] http://elbitsystems.com/Elbitmain/files/LILY-L.pdf
[24] Veprik, A., and Tuitto, A., "Multimodal tuned dynamic absorber for split Stirling linear cryocooler", Proc. SPIE. 9821, Tri-Technology Device Refrigeration (TTDR), 98210E (2016)
[25] Veprik, A., Tuitto, A., "Global vibration control of split Stirling linear cryogenic cooler", Proceedings ICC 19, 129-140 (2016)
[26] Stephen, N.G., "Vibration of a cantilevered beam carrying a tip heavy body by Dunkerley's method", Journal of Sound and Vibration, Volume 70, Issue 3, 463-465 (1980).
[27] Riabzev, S.V., Veprik, A.M., and Pundak, N., "Technical diagnostics of linear split stirling cryocooler through the analysis of self-induced forces", Advances in Cryogenic Engineering: Proceedings of the CEC, American Institute of Physics Vol. 47, CP613 (2002)